Talanta 221 (2021) 121483

Contents lists available at ScienceDirect

Talanta

journal homepage: www.elsevier.com/locate/talanta

A new ultralow fouling surface for the analysis of human plasma samples with surface plasmon resonance

Roberta D'Agata [a], Noemi Bellassai [a], Maria Chiara Giuffrida [b], Angela Margherita Aura [a], Christian Petri [c], Peter Kögler [c], Graziella Vecchio [a], Ulrich Jonas [c], Giuseppe Spoto [a,b,*]

[a] Dipartimento di Scienze Chimiche, Università Degli Studi di Catania, Viale Andrea Doria 6, Catania, Italy
[b] Consorzio Interuniversitario "Istituto Nazionale Biostrutture e Biosistemi", c/o Dipartimento di Scienze Chimiche, Università di Catania, Viale Andrea Doria 6, Catania, Italy
[c] Department Chemistry - Biology, University of Siegen, Adolf-Reichwein-Strasse 2, D-57076, Siegen, Germany

ARTICLE INFO

Keywords:
Surface plasmon resonance
Human plasma
Fouling
Betaine
Self-assembled monolayers
Disulfides

ABSTRACT

Surface plasmon resonance (SPR) has been widely used to detect a variety of biomolecular systems, but only a small fraction of applications report on the analysis of patients' samples. A critical barrier to the full implementation of SPR technology in molecular diagnostics currently exists for its potential application to analyze blood plasma or serum samples. Such capability is mostly hindered by the non-specific adsorption of interfering species present in the biological sample at the functional interface of the biosensor, often referred to as fouling. Suitable polymeric layers having a thickness ranging from 15 and about 70 nm are usually deposited on the active surface of biosensors to introduce antifouling properties. A similar approach is not fully adequate for SPR detection where the exponential decay of the evanescent plasmonic field limits the thickness of the layer beyond the SPR metallic sensor surface for which a sensitive detection can be obtained. Here, a triethylene glycol (PEG (3))-pentrimer carboxybetaine system is proposed to fabricate a new surface coating bearing excellent antifouling properties with a thickness of less than 2 nm, thus compatible with sensitive SPR detection. The high variability of experimental conditions described in the literature for the quantitative assessment of the antifouling performances of surface layers moved us to compare the superior antifouling capacity of the new pentrimeric system with that of 4-aminophenylphosphorylcholine, PEG-carboxybetaine and sulfobetaine-modified surface layers, respectively, using undiluted and diluted pooled human plasma samples. The use of the new coating for the immunologic SPRI biosensing of human arginase 1 in plasma is also presented.

1. Introduction

Molecular diagnostic plays a central role in modern medicine [1]. Molecular biomarkers are detected in biological fluids to diagnose and monitor the progression of important diseases. Biological fluids are also analyzed to assess the patient's response to therapy. A large number of analyses are performed using conventional analytical platforms. However, challenges still exist in the rapid detection of ultra-low concentrated analytes in complex body fluids such as blood. Biosensors have been shown to offer a credible alternative to conventional in vitro diagnostic platforms with great potential for the development of innovative detection methods able to meet the most challenging requirements [2]. Surface plasmon resonance (SPR) is an optical biosensing platform able to investigate biomolecular interactions in real-time and with high sensitivity [3]. SPR imaging (SPRI) expands the ability of SPR to detect analytes of clinical interest by allowing the multiplexed detection of molecular targets [4,5]. SPR has been used to detect a wide variety of biomolecular systems including nucleic acids, antibodies, enzymes, drugs and other molecular targets of clinical interest [6–9]. However, only about 1% of papers describing the use of SPR to detect analytes of clinical interest report on the analysis patients' samples [10]. A critical barrier to the full application of SPR technology in molecular diagnostics is represented by the limited capacity to analyze clinical samples such as blood plasma or serum. Such capability is mostly hindered by the non-specific adsorption of interfering species present in the biological medium at the functional interface of the biosensor, often referred to as fouling [11]. The minimization of the fouling on the sensor surface contributes to improving the sensitivity

* Corresponding author. Dipartimento di Scienze Chimiche, Università Degli Studi di Catania, Viale Andrea Doria 6, Catania, Italy.
E-mail address: spotog@unict.it (G. Spoto).

https://doi.org/10.1016/j.talanta.2020.121483
Received 6 March 2020; Received in revised form 23 July 2020; Accepted 29 July 2020
Available online 7 August 2020

and selectivity of the assay, thus allowing the analysis of low concentrated biomarkers in the biological fluid [12,13]. Until now, various materials able to minimize the fouling on surfaces have been identified [14]. They can be classified according to their chemical composition and include poly(ethylene glycol)/oligo(ethylene glycol)- (PEG/OEG)-based materials [15], zwitterionic compounds [16], and polysaccharide-based materials [17].

PEG-based materials are the most deeply investigated and widely adopted to fabricate antifouling coatings [18,19]. Polymeric materials bearing zwitterionic moieties, such as carboxybetaine (CB), sulfobetaine (SB) and phosphorylcholine (PC), have been put forward as an alternative to PEG polymers since they provide a high protein resistance in complex media, such as blood plasma and serum [20], with long-term stability in aqueous solutions and excellent biocompatibility [21,22]. However, preserving the antifouling activity of similar materials while introducing functionalities to immobilize biomolecular receptors for biosensing is still a challenge [23]. To overcome such constraint, the functionalization of three-dimensional polymer brushes not compromising the zwitterionic character and the antifouling property of the structure has been proposed [24].

Antifouling performances of hydrophilic polymers are tightly correlated with the formation of a water layer that prevents the non-specific adsorption of biomolecular entities on the surface [14]. In zwitterionic compounds, electrostatic forces are combined with the hydration layer to provide further resistance to protein adsorption [25]. Physicochemical properties, such as polymer chain flexibility, packing density, molecular weight and surface charge, also play a critical role in providing active antifouling materials [26,27].

The decay length (l_d) of the evanescent plasmonic field represents an essential parameter to consider when dealing with SPR biosensors. l_d limits the thickness of the layer beyond the metallic surface for which sensitive detection of analytes can be obtained. A reasonable estimate of l_d (37% of SPR wavelength) [28] provides a thickness of the SPR sensing layer at the level of a few hundreds of nanometers. However, the exponential decay of the field strength beyond the metallic surface of the SPR sensor makes layers closer to the gold surface better performing in terms of sensitive detection than further layers. For this reason, the frequent usage of antifouling polymeric layers having a thickness ranging from 15 and about 70 nm introduces a significant barrier to the development of highly sensitive SPR assays for the analysis of blood plasma or serum samples.

Here we present new surface functionalization protocols for the fabrication of anti-fouling layers having controlled thickness and thus better suited for sensitive SPR biosensing assays involving human plasma-based samples. In particular, we present surface functionalization procedures for the fabrication of a new PEG-pentrimer carboxybetaine-based layer with excellent anti-fouling capacity. The combination of PEG and carboxybetaine moieties with a dendrimer brush-like structure allows the accommodation of functional groups by keeping antifouling properties and limited thickness of the layer. We developed the new approach for the antifouling surface fabrication by also evaluating its compatibility with the standard protocols for the functionalization of gold chip surfaces used for SPR experiments.

The antifouling capacity of surfaces is often evaluated by quantifying with SPR [27] or other methods such as QCM [29] the mass of protein adsorbed when the surface comes in contact with single-protein buffered solutions (human serum albumin, fibrinogen, lysozyme are among the most abundant protein in the blood). Unfortunately, the reduced adsorption of a single type of protein does not imply the minimized fouling from the mixture of proteins available in blood-derived fluids [12,30]. Another issue to tackle when using blood-derived fluids to test antifouling performances refers to the different fouling usually observed on the same coating when blood plasma samples from different individual donors [30–32] are simultaneously analyzed. Such sample-to-sample variability is minimized with samples of pooled plasma [33].

A PEG-pentrimer carboxybetaine (PPCB) system is here proposed to fabricate new surface coatings bearing excellent antifouling properties with a thickness of less than 2 nm, thus compatible with sensitive SPR detection. The high variability of experimental conditions described in the literature for the quantitative assessment of the antifouling performances of surface layers moved us to compare the antifouling capacity of the new PEG-pentrimer carboxybetaine system with those of other surface layers compatible with the SPR requirements above discussed. With this aim, we tested with SPR and under the same experimental conditions antifouling performances of the systems shown in Fig. 1 using undiluted and diluted pooled human plasma samples.

We tested the capacity of PPCB to operate as an antifouling functional surface for SPR biosensing. With this aim, we used an immunological approach to detected human Arginase 1 in plasma and compared results obtained using surfaces with and without PPCB to highlight improvements of performances in biosensing obtained when analyzing plasma-based samples with PPCB surfaces.

Arginase is a trimeric metalloenzyme that converts L-arginine into L-ornithine and urea [34]. Arginase 1 is over-expressed in plasma of patients with lung, gastrointestinal and bladder cancers [35] and its expression level correlates with suppressed T-cell function and proliferation in patients with different histologies [36].

2. Experimental

2.1. Reagents, materials and apparatus

All chemicals and solvents were used without further purification. 3-Dimethylamino-1-propyne, beta-propiolactone, ethanol, dithiobis(N) succinimidylpropionate (DTSP), acetonitrile (CH_3CN), dimethyl sulfoxide (DMSO), tris(hydroxymethyl)aminomethane (Trizma) hydrochloride, and 11-azido-3,6,9-trioxaundecan-1-amine (NH_2-PEG-N_3), *N*-(3-dimethylaminopropyl)-*N*′-ethylcarbodiimide hydrochloride (EDC), *N*-hydroxysuccinimide (NHS), and 2-morpholinoethanesulfonic acid (MES) were purchased from Sigma-Aldrich (Milan, Italy). Hexadecaoxa-28,29-dithiahexapentacontanedioic acid di-*N*-succinimidyl ester (PEG (7)NHS ester disulfide or NHS-PEG-S) was purchased from Polypure (Oslo, Norway). Tetrahydrochloride PEG(3)-Pentrimer-G1-(NH_2+4N_3) *4HCl (NH_2-PP-4N_3, $C_{64}H_{125}N_{21}O_{20}$*4HCl, molecular weight 1508.81*145.81 g mol^{-1}, Fig. 2) was purchased from Iris Biotech GmbH (Marktredwitz, Germany). 4-Aminophenylphosphorylcholine (APPC) was obtained from Santa Cruz Biotechnology, Inc., Dallas, Texas, USA. Human plasma (SER-PLE Human Recovered Plasma Frozen. Anticoagulant: EDTA 200 mL) was purchased from ZenBio (North Carolina, USA). Mouse monoclonal antibodies (mAB-ARG1 *N*-term -sc-166920- and mAB-ARG1 C-term - sc-365547) against human Arginase 1 were purchased from Santa Cruz Biotechnology (DBA, Italy). Recombinant human Arginase 1 (ARG1) was purchased from Enzo Life Sciences (Milan, Italy) and supplied in 10 mM TRIS-HCl buffer, pH 7.5, containing 1 mM β-mercaptoethanol, 1 mM $MnCl_2$ and 50% glycerol. Phosphate buffered saline (PBS) (137 mM NaCl, 2.7 mM KCl, 10 mM phosphate buffer, pH 7.4) was obtained from Amresco (Italy). Carbonate-bicarbonate buffer was prepared by mixing sodium carbonate and sodium bicarbonate stock solutions and the pH of the buffer was adjusted to 10.2 using NaOH (0.1 M). We used ultrapure water produced with a Milli-Q Integral S3 system (Millipore, Italy) for all the experiments. SPRI gold substrates (Xantec bioanalytics GmbH, Germany) were washed with ultrapure water (Milli-Q water) and ethanol and dried with a stream of nitrogen gas. The substrates were cleaned with UV/ozone for 5 min, immersed in ethanol for 10 min and dried with a nitrogen stream.

2.2. PEG-carboxybetaine functionalized surface (PCB)

We functionalized gold chips with NHS-PEG-S (4 mM in DMSO, 2 days) (Fig. 1a). Then, we immersed sensor chips into a 4 mM solution of NH_2-PEG-N_3 in water for 3 h. Treatments with carbonate-bicarbonate

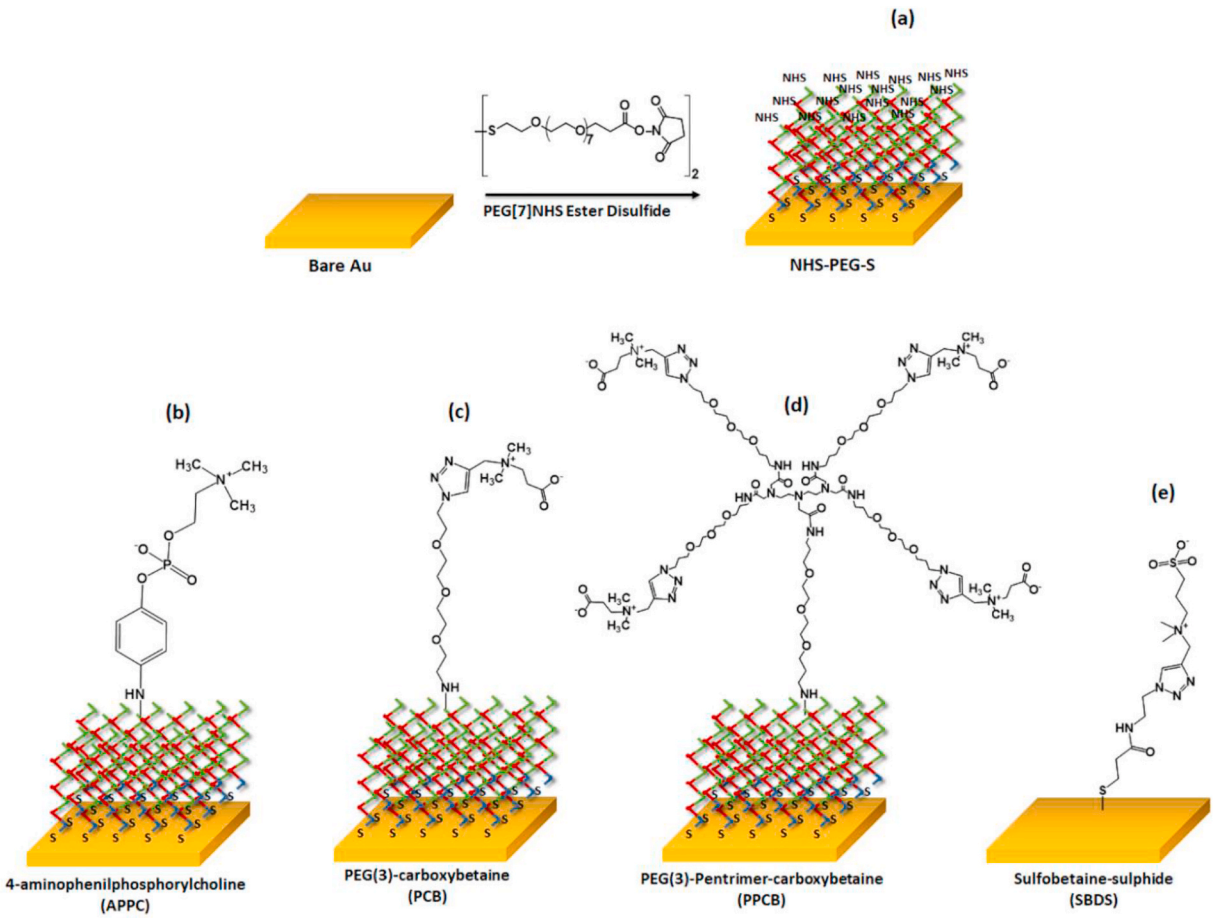

Fig. 1. Schematic diagram showing the different antifouling layers tested with SPR.

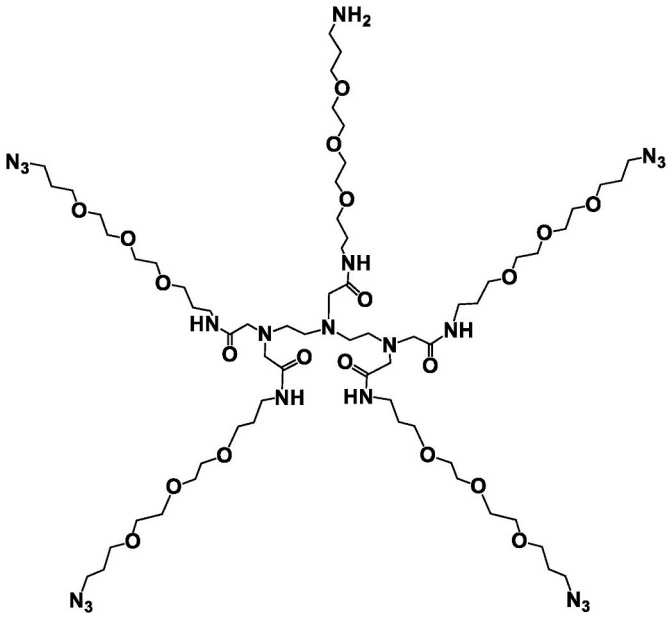

Fig. 2. Structure of PEG(3)-pentrimer-G1-(NH_2+4N_3) (NH_2-PP-4N_3).

buffer (pH = 10.2, 60 min) and Trizma hydrochloride solution (0.5 M in water, 45 min) followed to hydrolyze and deactivate unreacted NHS ester groups, respectively. We used some of the obtained chips directly for SPRI testing with human plasma and processed others by performing a click-chemistry reaction between the NH_2-PEG-N_3 modified surface and carboxybetaine alkyne **(1)** (Fig. 3) (4 mM in water) and CuBr(PPh_3)$_3$ (0.02 mM in water/t-BuOH, 2:1) for 2 h (Fig. 1c). We rinsed the sensor chips with water, ethanol, and dried them with nitrogen gas after each reaction step.

2.3. PEG(3)-pentrimer carboxybetaine functionalized surface (PPCB)

We functionalized gold chips with NHS-PEG-S (4 mM in DMSO, 2 days) (Fig. 1a) and the immersed them in NH_2-PP-4N_3 solution (4 mM in water) for 3 h. Afterwards, we treated chips with carbonate-bicarbonate buffer (pH = 10.2, 60 min) and Trizma hydrochloride (0.5 M in water, 45 min) to hydrolyze and deactivate unreacted NHS ester moieties, respectively. Cu-mediated click reaction was then performed using **(1)** (Fig. 3) (4 mM) and CuBr(PPh_3)$_3$ (0.02 mM in water/t-BuOH, 2:1) acting as a catalyst for a Copper(I)-catalyzed azide-alkyne cycloaddition for 2 h to obtain PEG(3)-pentrimer carboxybetaine-based compound (PPCB) (Fig. 1d). After each reactive step, we rinsed the modified surface with water and ethanol and dried it with nitrogen gas.

2.4. 4-Aminophenylphosphorylcholine (APPC) and sulfobetaine disulfide (SBDS) functionalized surfaces

We functionalized gold chips with NHS-PEG-S (4 mM in DMSO, 2 days) (Fig. 1a). Then we immersed them in an aqueous 4-aminophenyl-phosphorylcholine solution (4 mM) for 3 h. Before to use the APPC functionalized chips (Fig. 1b) for SPRI testing we soaked them in carbonate-bicarbonate buffer (pH = 10.2, 60 min) and Trizma hydrochloride solution (0.5 M in water, 45 min) to hydrolyze and deactivate unreacted NHS esters, respectively.

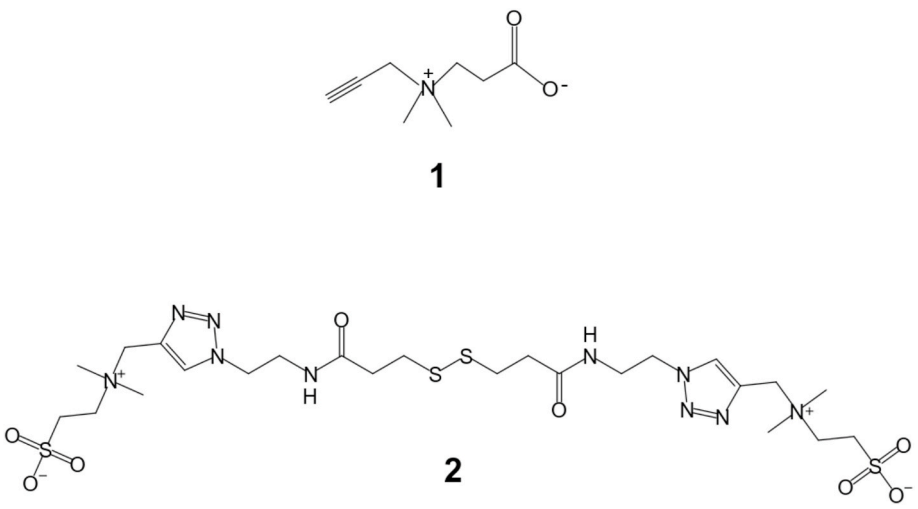

Fig. 3. Structure of (**1**) carboxybetaine alkyne (3-[dimethyl(prop-2-ynyl)ammonio]propanoate) and (**2**) sulfobetaine disulfide (SBDS). (Details on synthetic procedures are reported in Supplementary data).

We obtained sulfobetaine sulphide (SBDS) (**2**) (Fig. 3) functionalized surfaces immersing the bare gold chip in SBDS solution (1 mM in water) overnight. The modified chip was then rinsed with water and ethanol and dried with nitrogen. Full details of the synthesis and characterization of SBDS are provided in Supporting data.

2.5. SPRI experiments

SPR imager apparatus (GWC Technologies, U.S.A.) was used for SPRI experiments and V++ (version 4.0, Digital Optics Limited, New Zealand) and ImageJ 1.32j (National Institutes of Health, U.S.A.) software to analyze SPR images. SPRI experiments were conducted as elsewhere described [37] and obtained kinetic data by plotting the difference in percent reflectivity (Δ%R) from selected regions of interest (ROIs) of SPR images as a function of time. Changes of difference in percent reflectivity (Δ%R) were calibrated by measuring SPRI responses to NaCl water solutions (1%, 3% and 5%) with known refractive indices (n_c. 1.3347, 1.3383, 1.3418, respectively). The refractive index sensitivity ($S = \Delta\%R/\Delta n_c$) of the SPRI system is S = 6009.28 Δ%R/RIU.

Microfluidic devices, integrating six parallel channels (400 μm in width, 80 μm in depth) to independently perform different SPRI experiments for each functionalized chip were fabricated as elsewhere described [38].

We quantified the surface coverage of protein adsorbed on the functionalized surfaces after exposure to human plasma using SPRI. Experiments were conducted using pooled human plasma centrifuged at 16,000 g (10,800 rpm) for 10 min at 4 °C and its PBS solutions. Firstly, a stable SPR signal was established by flowing running buffer (PBS) for at least 5 min (flow rate 10 μL min^{-1}). Then, undiluted or diluted (in PBS) human plasma samples flowed for 30 min. During the last step of the SPRI experiment, we replaced the human plasma sample with PBS that was flowed for 10 min to wash off weakly adsorbed protein and to establish the final baseline. We quantified surface coverage (Γ, ng cm^{-2}) of protein adsorbed on the surface of the treated SPRI chips measuring the variation of Δ%R after the injection of the human plasma sample. The mass of adsorbate per unit area (ng cm^{-2}) was estimated on the basis of the theoretical model described by Shumaker-Parry et al. [39]. For the calculation, we considered specific density for human plasma protein $\rho_{PP} = 1.42$ g cm^{-3}, as the average value of the specific density of plasma proteins [40], the refractive index of plasma protein $n_{PP} = 1.53$ [41] and refractive index of PBS buffer $n_{PBS} = 1.33$. We also considered the decay length l_d as 37% of SPR wavelength [28].

We adopted the same theoretical model to quantify by SPRI the thickness of the layer obtained after the surface functionalization with NH_2-PEG-N_3, PCB, APPC and PPCB as already described. A different experimental procedure was instead adopted to evaluate the thickness of the layer obtained after treating for two days the gold surface with NHS-PEG-S (4 mM in DMSO). In this case, we detected with SPRI the NHS-PEG-S desorption from the gold surface induced by dithiothreitol (DTT, 100 mM in water, 2 h) [42]. For the calculation, we considered a refractive index n = 1.50 for the organic layer [43,44]. We calculated a thickness lower than 2 nm for all the investigated systems (Table 1). The thickness of SBDS layer was not calculated because it represents the smaller system among those we considered. The SPR shift detected after the surface functionalization was not large enough in the latter case to allow a reliable evaluation of the thickness of the layer.

2.6. SPRI biosensing of human arginase 1 using PPCB-functionalized surface

We immobilized mAB-ARG1 *N*-term antibody on PPCB surface to develop an SPRI biosensor for ARG1. With this aim, we activated the carboxyl group of carboxybetaine units of PPCB with EDC/NHS chemistry (0.4 M/0.1 M in MES) and immobilized the antibody by amine coupling. Experiments were performed at room temperature using a 10 μg mL^{-1} solution of mAB-ARG1 *N*-term capture antibody (30 min, flow rate 10 μL min^{-1}). After the immobilization, we washed the surface with PBS to remove reversibly adsorbed species. Unreacted NHS ester moieties were blocked with Trizma 0.5 M. To evaluate the specific contribution of the PPCB surface on ARG1 biosensing, we compared ARG1 biosensing on PPCB surface with biosensing on gold. In the latter case, we translated the same protocol already described for PPCB on gold surfaces functionalized with DTSP and mAB-ARG1 *N*-term (30 min, flow rate 10 μL min^{-1}) was immobilized on PPCB-free surface through amine coupling with *N*-succinimidyl-ester moieties of DTSP.

We used 1:10 diluted pooled plasma samples unspiked and spiked with ARG1 (12.5 nM, 50 nM) and a 12.5 nM solution of ARG1 in PBS to evaluate the biosensing capacity of PPCB surfaces. Those samples were adsorbed on mAB-ARG1 *N*-term for 30 min, then the surface was washed with PBS for 15 min.

We used mAB-ARG1 C-term antibody to confirm the specific detection of ARG1. mAB-ARG1 C-term was raised against amino acids 271–322 close to C-terminus of human Arginase 1. mAB-ARG1 *N*-term is instead specific for an epitope mapping between amino acids 46–65 near the *N*-terminus of human Arginase 1. In the last step of the assay, we adsorbed mAB-ARG1 C-term (10 μg mL^{-1} in PBS) for 15 min (flow rate 8 μL min^{-1}) that interacted with a region of ARG1 not involved in the interaction with the surface immobilized mAB-ARG1 *N*-term antibody.

Table 1
Antifouling materials and the corresponding values of the mass of protein adsorbed per unit area (Γ) after treatment of the surface with human plasma. Γ values obtained from SPR experiments. The thickness of the antifouling layer and the time of the plasma adsorption are also shown.

Antifouling materials		Γ (ng cm^{-2})	Antifouling layer thickness (nm)	Adsorption time (min)	Refs.
	Bare Au	307	0	75	[52]
PEG/OEG	Carboxy-capped tri(ethylene glycol) undecanethiol	105	2.1	30	[53]
	11-azido-3,6,9-trioxaundecan-1-amine (NH_2-PEG-N_3)	148.5	<2	30	this work
	Poly(oligo(ethylene glycol) methyl ether methacrylate)	48	27.3	30	[53]
Betaines	Polycarboxybetaine acrylamide (ATRP)	<5	15–25	10	[20]
	Polycarboxybetaine acrylamide (SIP)	4.2	25.6	10	[49]
	Poly(sulfobetaine methacrylate)	6.09	62	15	[48]
	3,3′-disulfanediylbis(*N*-(2-azidoethyl)propanamide (SBDS)	203.4	–	30	this work
	PEG(3)-carboxybetaine-based-compound (PCB)	35.8	<2	30	this work
	PEG(3)-Pendrimer carboxybetaine (PPCB)	2.4	<2	30	this work
Phosphoryl cholines	Poly[(methacrylic acid)-ran-(2-methacryloyloxyethyl phosphoryl-choline)]	~20	~8	15	[54]
	2-Methacryloyloxyethyl phosphorylcholine	~200	–	15	[25]
	4-aminophenilphosphoryl choline (APPC)	264.9	<2	30	this work
Polypeptides	Poly(lysine methacrylamide)	5.4	14.5	10	[55]
	Poly(serine methacrylate)	12.9	37.2	10	[56]
	poly-L-lysine polymers with anionic oligopeptide side-chains	48	7.5	10	[57]

3. Results and discussion

Fig. 1 depicts the surface functionalization approaches we have designed and tested to identify the best strategy to fabricate antifouling surfaces for SPR analysis of human plasma samples. We exploited zwitterionic structures to improve the surface resistance to the adsorption of human plasma components and designed functionalization procedures for the fabrication of antifouling layers having controlled thickness, thus allowing the design of sensitive SPR biosensing assays. As we already pointed out, the exponential decay of the field strength beyond the metallic surface makes the region close to the gold surface better performing in terms of SPR sensitive detection than further layers.

Protocols we designed to functionalize the gold surface of SPR sensors comprise incubation in PEG(7)NHS ester disulfide solution for 2 days leading to the formation of NHS-PEG-S layer exposing reactive NHS moieties as a consequence of bonds established between Au surface and disulfide groups (Fig. 1a). We used NHS ester moieties to extend the layer by moieties bearing zwitterionic units through a simple amine coupling reaction. In particular, we produced different zwitterionic layers using i) APPC (Fig. 1b), ii) PCB (Fig. 1c) or iii) PPCB (Fig. 1d) compounds. A simplified approach for the surface functionalization with zwitterionic groups was also considered by treating Au surface with SBDS (Fig. 1e).

We tested the antifouling capacity of surface coatings measuring the change of the SPRI signal produced by the running buffer (PBS) after the surface exposure (30 min) to undiluted or diluted (1:5, 1:10 in PBS) pooled human plasma samples. Molecular species non specifically adsorbed on the surface are responsible for the detected SPRI signal change and, for this reason, we converted the measured SPRI change into the mass of adsorbate per unit area (ng cm^{-2}) on the basis of the theoretical model described elsewhere [39]. We used samples of pooled plasma instead of plasma from a single donor to minimize the sample to sample variability usually found when human plasma samples from different donors are analyzed [45].

The simplest surface functionalization protocol we designed and tested has been based on the direct immobilization of SBDS on Au (Fig. 1e). The adsorption of SBDS on Au results in a stable interaction between the disulfide moiety and Au thus providing, after only a single functionalization step, a surface layer exposing sulfobetaine moieties.

The capacity of selected polymeric structures bearing sulfobetaine units to minimize non-specific adsorption of components from blood-derived fluids has been already investigated [46,47].

Fig. 4 shows SPR sensorgrams we detected when testing the antifouling capacity of SBDS modified gold surfaces with undiluted and 1:5 and 1:10 diluted human plasma. We observed the saturation of the detected SPR signal while undiluted human plasma samples were adsorbed on the modified surface. 1:5 and 1:10 diluted plasma samples instead produced changes in percent reflectivity (Δ%R) at the level of 27.9 (change in refractive index units, RIU = 4.6 10^{-3}) and 19.3 (RIU = 3.2 10^{-3}), respectively. We quantified the mass of non specifically adsorbed protein per unit area, considering Δ%R values after stable SPRI responses were detected when the PBS running buffer replaced plasma samples (Fig. 3 t = 2500 s). In particular, we identified a stable SPR signal at Δ%R = 16.8 after the adsorption of undiluted human plasma and at Δ%R = 12.8 and Δ%R = 11.3 after the adsorption of 1:5 and 1:10 diluted plasma samples, respectively. We determined the coverage of SBDS-modified Au surfaces by non specifically adsorbed plasma protein considering the latter Δ%R values. Γ_{SBDS} = 203.4 ng cm^{-2} was

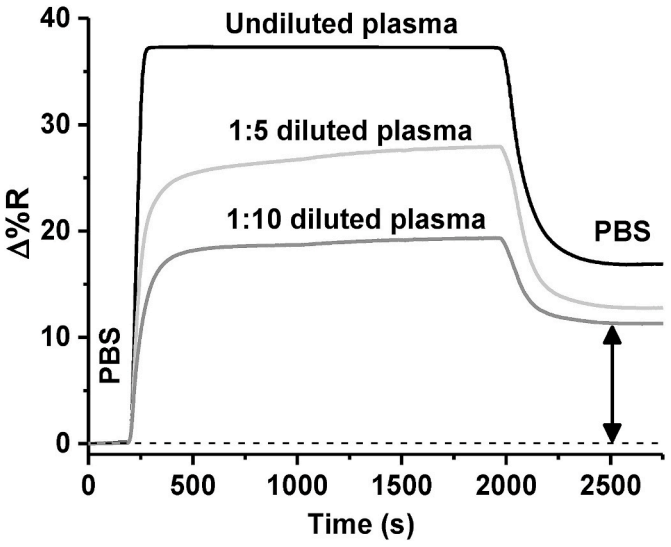

Fig. 4. Time-dependent SPRI curves obtained after the adsorption of undiluted plasma (black curve), diluted plasma (1:5) (light gray curve), diluted plasma (1:10) (dark gray curve) on a sulfobetaine-functionalized surface (SBDS).

determined for 1:10 diluted human plasma.

When we applied the same protocol to assess the surface layer obtained after the amine coupling of APPC with NHS-PEG-S layer formed on the Au surface (Fig. 1b), Δ%R values corresponding to 22.9, 18.5 and 15.9 were measured for undiluted, 1:5 diluted and 1:10 diluted plasma samples, respectively. Δ%R value we measured after the adsorption of 1:10 diluted plasma (t = 2500 s) corresponds to $\Gamma_{APPC} = 264.9$ ng cm^{-2} of protein adsorbed on the modified surface.

We obtained the best antifouling performances when surface functionalization protocols involving carboxybetaine units were designed and used. We developed protocols to produce surface geometries compatible with the requirements for both the thickness of the SPR sensitive layer as well as the simplicity of the functionalization procedures and stability of the formed antifouling layer.

We fabricated PCB functionalized gold surfaces modifying the Au-immobilized NHS-PEG-S layer through amine coupling with NH_2-PEG-N_3, then we introduced carboxybetaine alkyne **(1)** groups with a click-chemistry reaction (Fig. 1c). The final surface architecture comprised a PEG-based layer with carboxybetaine end groups. To assess the role played by carboxybetaine in improving the antifouling capacity of the surface layers, we compared SPRI kinetic data referring to the adsorption of human plasma samples on surfaces functionalized without and with the zwitterionic carboxybetaine groups. Fig. 5a shows representative SPRI kinetic data related to the adsorption of undiluted and 1:5 and 1:10 diluted human plasma samples, respectively, on the layer obtained after NH_2-PEG-N_3 coupling to NHS-PEG-S. Fig. 5b instead refers to the adsorption of the plasma samples on surface layers modified with also carboxybetaine groups (Fig. 1c. PCB). The comparison of SPRI responses detected after the signal stabilization with PBS running buffer (t = 2500 s) provided us with the evidence of the critical role played by zwitterionic carboxybetaine groups on the antifouling capacity of the surface layer. In particular, Δ%R values of 2.0 (RIU = 3.3 10^{-4}) and 8.2 (RIU = 1.4 10^{-3}) have been measured after the adsorption of 1:10 diluted plasma samples on the modified surface layers with and without carboxybetaine groups, respectively. Such responses correspond to $\Gamma_{PCB} = 35.8$ ng cm^{-2} and $\Gamma_{N_H2\text{-}PEG\text{-}N3} = 148.5$ ng cm^{-2} of protein adsorbed after 30 min of diluted plasma adsorption on surfaces with and without carboxybetaine groups, respectively.

Antifouling properties of surface layers are correlated with their capacity to bind water molecules forming a stable hydration layer. Such layer contributes to minimizing the release of water molecules from both the surface and the adsorbed protein that reduces the free energy barrier, thus favouring the non-specific adsorption. The flexibility of the surface layer also plays an essential role in determining antifouling properties because the compression of the layer by protein causes steric repulsion [14]. The above-reported considerations moved us to design a new surface functionalization approach based on a pentavalent dendrimer system (Fig. 2) bearing one amino and four azido functions. After amine coupling of NH_2-PP-4N_3 with the NHS-PEG-S layer formed on the Au surface, we introduced carboxybetaine alkyne (1) via click-chemistry reaction to obtain PPCB (Fig. 1d). The resulting PPCB system alters the ratio between zwitterionic and ethylene glycol units compared to PCB. It also enhances the flexibility of the surface layer. Also in this case, we tested the antifouling performances of the new surface layer by measuring changes of the running buffer (PBS) SPRI baseline after 30 min exposure to undiluted and diluted (1:5, 1:10 in PBS) human plasma samples.

Fig. 6 shows representative SPRI sensorgrams we detected. Δ%R values after the signal stabilization with PBS running buffer (t = 2500 s) were 4.6 (RIU = 8.0 10^{-4}), 1.1 (RIU = 1.8 10^{-4}) and 0.1 (RIU = 1.7 10^{-5}) for undiluted, 1:5 diluted and 1:10 diluted plasma samples, respectively. The Δ%R value we measured after the adsorption of 1:10 diluted plasma (t = 2500 s) corresponds to $\Gamma_{PPCB} = 2.4$ ng cm^{-2} of protein adsorbed on the PPCB-modified surface.

Fig. 7 summarizes SPRI responses we detected with running buffer after the exposure of the studied surface layers to human plasma

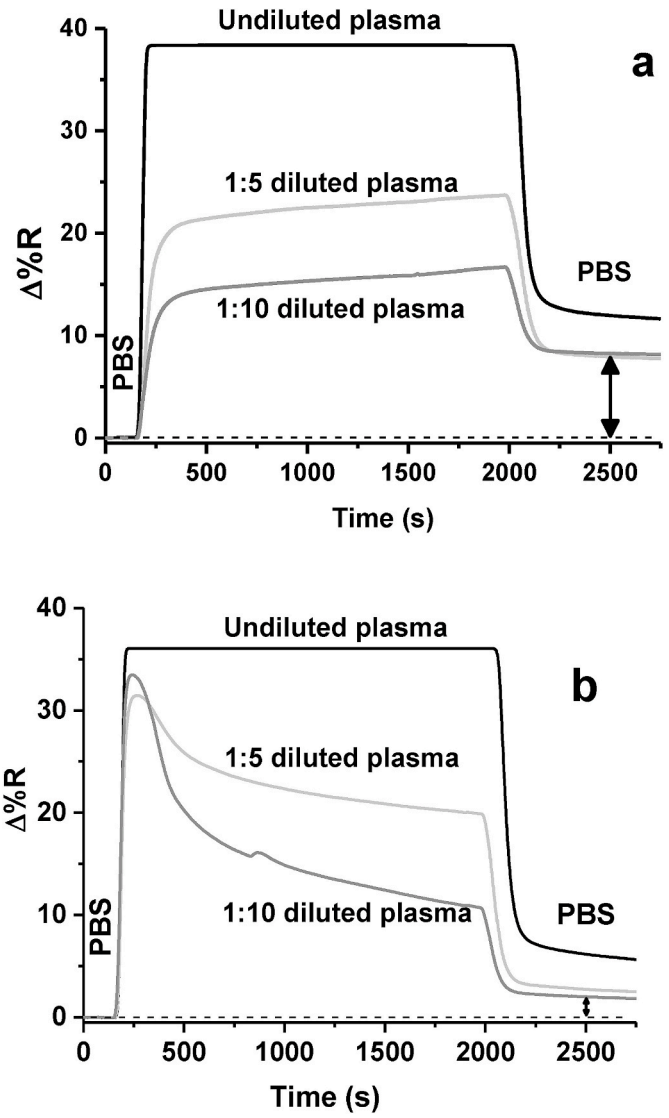

Fig. 5. Time-dependent SPRI curves obtained after the adsorption of undiluted plasma (black curve), diluted plasma (1:5) (light gray curve), diluted plasma diluted (1:10) (dark gray curve) on **a**) NH_2-PEG-N_3 and **b**) PEG(3)-carboxybetaine (PCB) functionalized surface.

samples. The changes are proportional to the mass of non specifically adsorbed plasma-derived species on the surface. Therefore, the lowest detected SPRI signal corresponds to the better performing antifouling surface layer. The newly designed surface geometry based on the pentrimeric PEG structure bearing carboxybetaine zwitterionic end-groups (PPCB) has shown the best antifouling performances (Fig. 7, black spheres). Table 1 shows Γ values for the investigated surfaces when treated with pooled human plasma for 30 min. Table 1 also aims at comparing the antifouling properties of the plasma-treated surface coatings here described with antifouling layers already described in the literature. Unfortunately, a straightforward comparison with data available in the literature is not readily achievable. In fact, SPR experiments performed to assess the antifouling capacity of surface coatings described in the literature are often conducted using different experimental conditions. Different surface exposure times to the plasma sample and, more importantly, different treatments of the plasma before the analysis introduces high variability in the final SPR responses thus influencing the surface coverage calculated values. The vast majority of papers discussing SPR data referring to the adsorption of human plasma on antifouling surfaces do not provide details on procedures adopted to

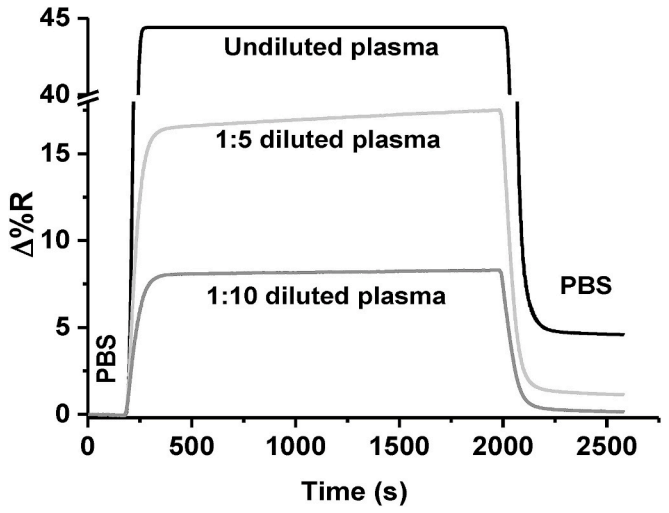

Fig. 6. Time-dependent SPRI curves obtained after the adsorption of undiluted plasma (black curve), diluted plasma (1:5) (light gray curve), diluted plasma (1:10) (dark gray curve) on PPCB functionalized surface.

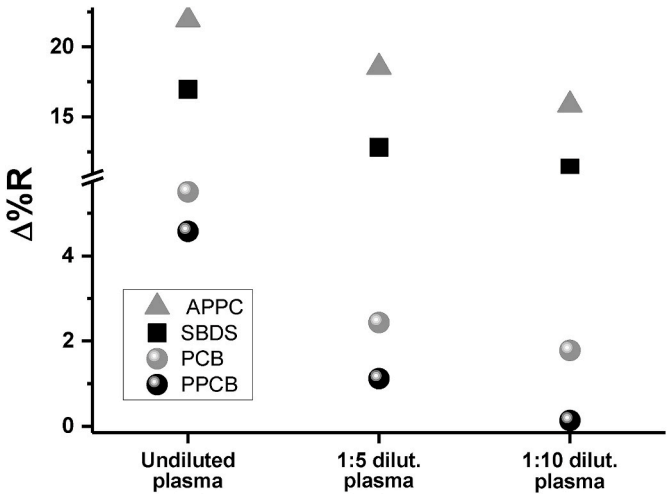

Fig. 7. SPRI responses in terms in percent reflectivity (Δ%R) obtained for the APPC-(triangles), SBDS- (squares) PCB-(gray spheres) and PPCB- surface (black spheres) after the exposure to human plasma samples.

isolate plasma from whole blood (e.g. type of anticoagulant, information on the centrifugation steps) and only a few papers refer to experiments conducted with pooled plasma samples [20,48,49]. Some authors did not use pure plasma samples, plasma solutions are instead used for the tests. For this reason, Table 1 reports results we obtained using 1:10 diluted plasma samples to compare the performances of the surface layers we designed with published data referring to antifouling materials tested under similar conditions. More than 10-fold diluted plasma samples can provide low protein adsorption; however, the relevance for practical use of antifouling surfaces tested with highly diluted plasma samples may be limited [50]. For example, the detection of ultra-low concentrated cancer biomarkers circulating in body fluids is essential for the implementation of diagnostic assays based on liquid biopsy samples [2,51]. The use of highly diluted plasma samples may prevent the detection of ultra-low concentrated biomarkers, thus affecting the capacity to perform effective detection of the selected biomarkers.

An essential aspect to consider to correctly assess possibilities offered by the PPCB dendrimeric system in fabricating antifouling surfaces for SPR-based assays of human plasma samples is represented by the balance between the antifouling capacity (low Γ value), the small thickness of the antifouling layer (<2 nm) and the simple implementation of the gold chip surface modification protocol to obtain an antifouling layer having limited thickness. The latter aspect constitutes a substantial difference with methods using polymerization reactions such as atom transfer radical polymerization (ATRP) [20] or surface-initiated polymerization (SIP) by photoirradiation to fabricate carboxybetaine-based antifouling polymeric layers [49]. Polycarboxybetaine acrylamide layers assembled by ATRP or SIP shows excellent antifouling performances ($\Gamma < 5$ ng cm^{-2}) and thickness that can reach 25 nm. Similar thicknesses significantly affect the sensitivity of SPR detection.

We develop an SPRI immunosensor for human Arginase 1 to show that a biosensor can be formed with the use of PPCB and highlight advantages of such a system over one without PPCB. We immobilized mAB-ARG1 *N*-term antibody on PPCB through amine coupling with carboxyl groups of carboxybetaine units. Carboxyl groups were activated with EDC/NHS before the immobilization. mAB-ARG1 *N*-term is a monoclonal antibody that specifically interacts with an epitope of ARG1 near the *N*-terminus (amino acids 46–65). Fig. 8 shows a representative SPRI sensorgram we detected for the immobilization.

To evaluate the capacity of the PPCB-based biosensor to detect ARG1, we compared SPRI responses for the adsorption of plasma samples spiked with ARG1 (12.5 nM, 50 nM) with those obtained for unspiked plasma and ARG1 in PBS buffer (12.5 nM) (Fig. 9).

SPRI signals detected after the adsorption of spiked and unspiked plasma samples were in line with the different ARG1 concentrations, and the comparison of responses detected with plasma samples and the ARG1 solution in PBS buffer allows to evaluate the significant impact played by the plasma matrix on the detected signal (Fig. 9). SPRI responses detected during the adsorption of the spiked (50 nM and 12.5 nM, respectively) and unspiked plasma samples were produced by ARG1 and the other components included in ARG1 mother solution (10 mM TRIS-HCl buffer, 1 mM β-mercaptoethanol, 1 mM $MnCl_2$ and 50% glycerol). Such components contributed to the SPRI signals detected when switching from the PBS running buffer to ARG1 solution. They adsorb on the surface of the biosensor, thus potentially contributing to the generation of the different responses we detected when the PBS baseline was established after ARG1 adsorption. For this reason, we used mAB-ARG1 C-term antibody to confirm the specific detection of ARG1 (Fig. 10). mAB-ARG1 C-term antibody interacts with an epitope of ARG1 close to C-terminus (amino acids 271–322) and not involved in the interaction with the surface-immobilized mAB-ARG1 *N*-term antibody.

We replicated the same analytical approach using bare gold surfaces to evaluate the role played by PPCB on the specific detection of ARG1 in plasma. We used DTSP-functionalized gold surfaces to immobilize mAB-

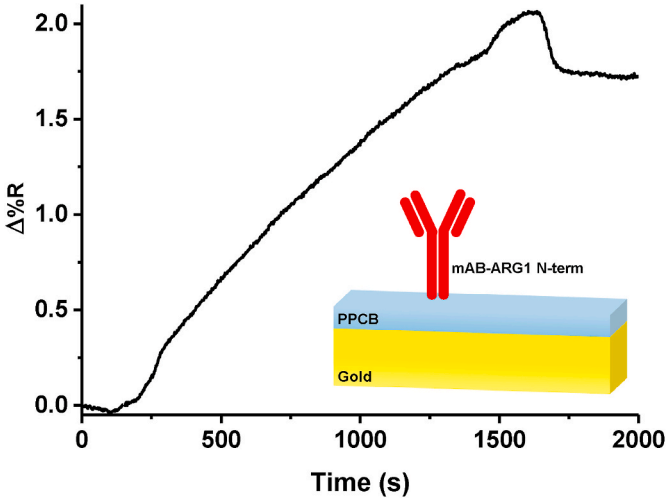

Fig. 8. Time-dependent SPRI curves obtained for the immobilization of mAB-ARG1 *N*-term (10 μg mL^{-1}) on EDC/NHS activated PPCB.

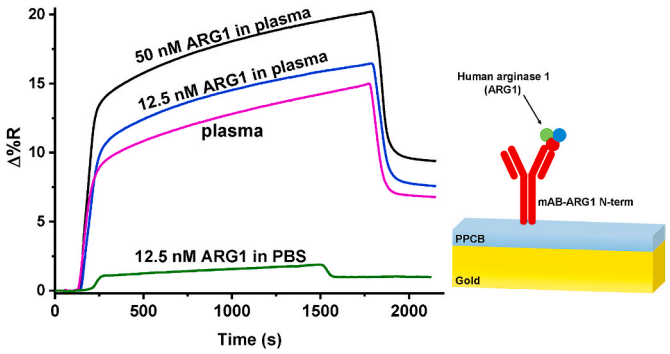

Fig. 9. Time-dependent SPRI curves obtained for the adsorption of ARG1 spiked plasma samples (12.5 nM, 50 nM), unspiked plasma and a 12.5 nM solution of ARG1 in PBS buffer on mAB-ARG1 *N*-term covalently immobilized on PPCB.

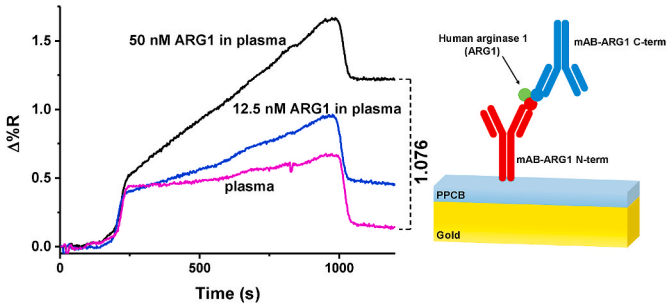

Fig. 10. Time-dependent SPRI curves obtained for the adsorption of mAB-ARG1 C-term on surfaces resulting from the adsorption of spiked (ARG1. 12.5 nM, 50 nM) and unspiked plasma samples on mAB-ARG1 *N*-term covalently immobilized on PPCB.

ARG1 *N*-term antibody through amine coupling reaction. Fig. 11 shows SPRI kinetic profiles for the adsorption of ARG1 spiked (12.5 nM, 50 nM) and unspiked plasma samples and a solution of ARG1 in PBS buffer (12.5 nM). Whereas no significant differences were observed in SPRI responses for the solution of ARG1 in PBS compared to experiments performed on PPCB (Fig. 9), responses detected for plasma solutions highlighted the different properties of the surfaces. In particular, higher Δ%R values, resulting from the non-specific adsorption of plasma components on the surface, were detected when the running buffer baseline were acquired after the adsorption of unspiked and spiked plasma solutions on gold compared to PPCB surface. Moreover, responses not in line with ARG1 concentration were detected (Fig. 11b), likely due to the interaction of components of ARG1 mother solution, which include β-mercaptoethanol that spontaneously chemisorbs on gold, with the DTSP functionalized gold surface. The direct detection of ARG1 in plasma was then not useful to achieve a correct evaluation of ARG1 concentration and discrimination between spiked and unspiked samples when the PPCB-free surface was used.

The adsorption of mAB-ARG1 C-term antibody was also affected by the surface instability resulting from the adsorption of components of plasma-based samples of the PPCB-free surface, as testified by the negative drift of the SPRI signal visible in Fig. 12. The SPRI detection of the interaction between ARG1 adsorbed on the primary antibody and mAB-ARG1 C-term antibody recovered the correct correlation between ARG1 concentrations and Δ%R values, but with SPRI signals close to the instrumental noise. A difference corresponding to $\Delta\%R = 0.236$ was measured between PBS baselines for 50 nM ARG1 spiked plasma and unspiked plasma (Fig. 12), whereas $\Delta\%R = 1.076$ was measured for the same samples when using PPCB surface (Fig. 10), thus further testifying the better analytical performance of the PPCB surface over DTSP-functionalized gold surface.

4. Conclusions

The PPCB-based surface functionalization here presented offers new opportunities for the fabrication of antifouling layers for SPR experiments based on human plasma samples. The thickness of the antifouling layer is an often under-estimated issue when dealing with SPR detection of analytes in complex biological samples. Such an issue introduces even more stringent limitations when using localized SPR (LSPR) for the analysis of human plasma samples due to the much smaller decay length of the electromagnetic field induced by LSPR compared to propagating SPR [58]. The presented method provides a convenient way to fabricate

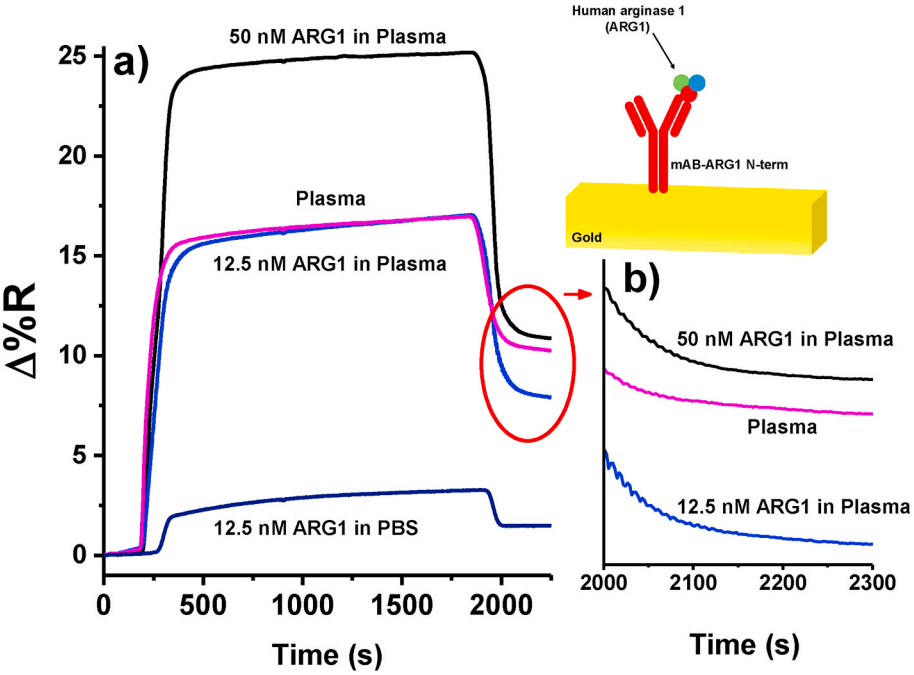

Fig. 11. a) Time-dependent SPRI curves obtained for the adsorption of ARG1 spiked plasma samples (12.5 nM, 50 nM), unspiked plasma and a 12.5 nM solution of ARG1 in PBS buffer on mAB-ARG1 *N*-term covalently immobilized on DTSP-functionalized gold surfaces. b) An SPR response not in line with ARG1 concentration is detected when PBS buffer is run after the adsorption of plasma-based samples. (For interpretation of the references to colour in this figure legend, the reader is referred to the Web version of this article.)

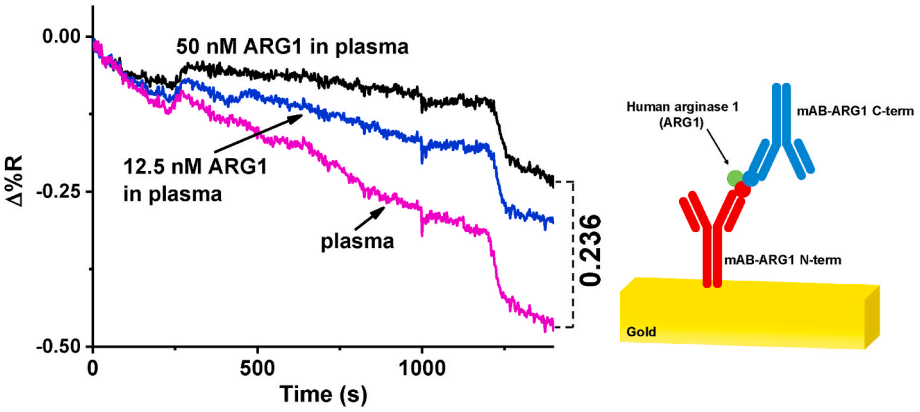

Fig. 12. Time-dependent SPRI curves obtained for the adsorption of mAB-ARG1 C-term on surfaces resulting from the adsorption of spiked (ARG1. 12.5 nM, 50 nM) and unspiked plasma samples on mAB-ARG1 *N*-term covalently immobilized on DTSP-functionalized gold surfaces. (For interpretation of the references to colour in this figure legend, the reader is referred to the Web version of this article.)

effective antifouling surface layers with a thickness of less than 2 nm, thus compatible with sensitive SPR and LSPR detection. SPR experiments here presented showed that the dendrimeric PPCB structure provides excellent antifouling resistance to nonspecific adsorption of proteins from 1:10 diluted, pooled human plasma ($\Gamma_{PPCB} = 2.4$ ng cm^{-2}). PPCB also represents a suitable functional platform for SPR biosensing of biomolecular analytes in human plasma. In particular, ARG1 in plasma is detected with an immunological approach more efficiently when using a PPCB modified surface compared to a PPCB-free surface. The comparison of antifouling performances of different molecular systems tested under the same experimental conditions here provided offers indications for the future development of antifouling coatings compatible with the challenging requirements of plasmonic platforms able to detect ultralow concentrated biomarkers in peripheral blood.

Credit author statement

Roberta D'Agata: Conceptualization, Methodology, Data curation, Investigation, Writing - original draft. Noemi Bellassai: Methodology, Data curation, Investigation, Visualization, Writing - original draft. Maria Chiara Giuffrida: Conceptualization, Methodology, Data curation, Investigation. 2, Angela Margherita Aura: Conceptualization, Methodology, Data curation, Investigation. Christian Petri: Methodology, Investigation. Peter Kögler: Methodology, Investigation. Graziella Vecchio: Methodology, Investigation. Ulrich Jonas: Methodology, Funding acquisition, Writing - review & editing. Giuseppe Spoto: Conceptualization, Funding acquisition, Supervision, Project administration, Writing - review & editing.

Declaration of competing interest

The authors declare that they have no known competing financial interests or personal relationships that could have appeared to influence the work reported in this paper.

Acknowledgment

We acknowledge support from the European Union's Horizon 2020 research and innovation programme under grant agreements n. 633937, project ULTRAPLACAD and from MIUR Prin 2017 (n. 2017RHX2E4).

Appendix A. Supplementary data

Supplementary data to this article can be found online at https://doi.org/10.1016/j.talanta.2020.121483.

References

[1] F.S. Collins, H. Varmus, A new initiative on precision medicine, N. Engl, J. Med. 372 (2015) 793–795, https://doi.org/10.1056/NEJMp1500523.
[2] N. Bellassai, G. Spoto, Biosensors for liquid biopsy: circulating nucleic acids to diagnose and treat cancer, Anal. Bioanal. Chem. 408 (2016) 7255–7264, https://doi.org/10.1007/s00216-016-9806-3.
[3] J. Homola, Surface plasmon resonance sensors for detection of chemical and biological species, Chem. Rev. 108 (2008) 462–493, https://doi.org/10.1021/cr068107d.
[4] G. Spoto, M. Minunni, Surface plasmon resonance imaging: what next? J. Phys. Chem. Lett. 3 (2012) 2682–2691, https://doi.org/10.1021/jz301053n.
[5] R. D'Agata, G. Spoto, Surface plasmon resonance imaging for nucleic acid detection, Anal. Bioanal. Chem. 405 (2013) 573–584, https://doi.org/10.1007/s00216-012-6563-9.
[6] R. D'Agata, G. Breveglieri, L.M. Zanoli, M. Borgatti, G. Spoto, R. Gambari, Direct detection of point mutations in nonamplified human genomic DNA, Anal. Chem. 83 (2011) 8711–8717, https://doi.org/10.1021/ac2021932.
[7] P. Palladino, M. Minunni, S. Scarano, Cardiac Troponin T capture and detection in real-time via epitope-imprinted polymer and optical biosensing, Biosens. Bioelectron. 106 (2018) 93–98, https://doi.org/10.1016/j.bios.2018.01.068.
[8] G. Grasso, A.I. Bush, R. D'Agata, E. Rizzarelli, G. Spoto, Enzyme solid-state support assays: a surface plasmon resonance and mass spectrometry coupled study of immobilized insulin degrading enzyme,, Eur. Biophys. J. 38 (2009) 407–414, https://doi.org/10.1007/s00249-008-0384-y.
[9] J.P. Renaud, C.W. Chung, U.H. Danielson, U. Egner, M. Hennig, R.E. Hubbard, H. Nar, Biophysics in drug discovery: impact, challenges and opportunities, Nat. Rev. Drug Discov. 15 (2016) 679–698, https://doi.org/10.1038/nrd.2016.123.
[10] J.-F. Masson, Surface plasmon resonance clinical biosensors for medical diagnostics, ACS Sens. 2 (2017) 16–30, https://doi.org/10.1021/acssensors.6b00763.
[11] I. Banerjee, R.C. Pangule, R.S. Kane, Antifouling coatings: recent developments in the design of surfaces that prevent fouling by proteins, bacteria, and marine organisms, Adv. Mater 23 (2011) 690–718, https://doi.org/10.1002/adma.201001215.
[12] C. Blaszykowski, S. Sheikh, M. Thompson, Surface chemistry to minimize fouling from blood-based fluids, Chem. Soc. Rev. 41 (2012) 5599–5612, https://doi.org/10.1039/c2cs35170f.
[13] M. Thompson, C. Blaszykowski, S. Sheikh, C. Rodriguez-Emmenegger, A. de los Santos Pereira, Antifouling Surface Chemistries to Minimize Signal Interference from Biological Matrices in Biosensor Technology, in: Biol. Fluid–Surface Interact, Royal Society of Chemistry, 2017, pp. 184–265, https://doi.org/10.1039/9781782622048-00184. Detect. Med. Devices.
[14] S. Chen, L. Li, C. Zhao, J. Zheng, Surface hydration: principles and applications toward low-fouling/nonfouling biomaterials, Polymer 51 (2010) 5283–5293, https://doi.org/10.1016/J.POLYMER.2010.08.022.
[15] J.M. Harris, Introduction to biotechnical and biomedical applications of poly (ethylene glycol), in: Poly(Ethylene Glycol) Chem., Springer US, 1992, pp. 1–14, https://doi.org/10.1007/978-1-4899-0703-5_1. Boston, MA.
[16] Q. Shao, S. Jiang, Molecular understanding and design of zwitterionic materials, Adv. Mater 27 (2015) 15–26, https://doi.org/10.1002/adma.201404059.
[17] X. Liu, R. Huang, R. Su, W. Qi, L. Wang, Z. He, Grafting hyaluronic acid onto gold surface to achieve low protein fouling in surface plasmon resonance biosensors, ACS Appl. Mater. Interfaces 6 (2014) 13034–13042, https://doi.org/10.1021/am502921z.
[18] L. Li, S. Chen, J. Zheng, B.D. Ratner, S. Jiang, Protein adsorption on oligo(ethylene glycol)-terminated alkanethiolate self-assembled monolayers: the molecular basis for nonfouling behavior,, J. Phys. Chem. B 109 (2005) 2934–2941, https://doi.org/10.1021/jp0473321.

[19] E. Ostuni, R.G. Chapman, R.E. Holmlin, S. Takayama, G.M. Whitesides, A survey of structure-property relationships of surfaces that resist the adsorption of protein,, Langmuir 17 (2001) 5605–5620, https://doi.org/10.1021/la010384m.

[20] H. Vaisocherová, Z. Zhang, W. Yang, Z. Cao, G. Cheng, A.D. Taylor, M. Piliarik, J. Homola, S. Jiang, Functionalizable surface platform with reduced nonspecific protein adsorption from full blood plasma-Material selection and protein immobilization optimization, Biosens. Bioelectron. 24 (2009) 1924–1930, https://doi.org/10.1016/j.bios.2008.09.035.

[21] A.T. Nguyen, J. Baggerman, J.M.J. Paulusse, C.J.M. Van Rijn, H. Zuilhof, Stable protein-repellent zwitterionic polymer brushes grafted from silicon nitride, Langmuir 27 (2011) 2587–2594, https://doi.org/10.1021/la104657c.

[22] J.C. Kim, M. Kim, J. Jung, H. Kim, I.J. Kim, J.R. Kim, M. Ree, Biocompatible characteristics of sulfobetaine-containing brush polymers, Macromol. Res. 20 (2012) 746–753, https://doi.org/10.1007/s13233-012-0099-x.

[23] S. Demirci, S. Kinali-Demirci, S. Jiang, A switchable polymer brush system for antifouling and controlled detection,, Chem. Commun. 53 (2017) 3713–3716, https://doi.org/10.1039/c7cc00193b.

[24] S.C. Lange, E. van Andel, M.M.J. Smulders, H. Zuilhof, Efficient, Tunable Three-Dimensional, Functionalization of fully zwitterionic antifouling surface coatings, Langmuir 32 (2016) 10199–10205, https://doi.org/10.1021/acs.langmuir.6b02622.

[25] T. Goda, M. Tabata, M. Sanjoh, M. Uchimura, Y. Iwasaki, Y. Miyahara, Thiolated 2-methacryloyloxyethyl phosphorylcholine for an antifouling biosensor platform, Chem. Commun. 49 (2013) 8683–8685, https://doi.org/10.1039/c3cc44357d.

[26] G. Gunkel, M. Weinhart, T. Becherer, R. Haag, W.T.S. Huck, Effect of polymer brush architecture on antibiofouling properties, Biomacromolecules 12 (2011) 4169–4172, https://doi.org/10.1021/bm200943m.

[27] B. Liu, X. Liu, S. Shi, R. Huang, R. Su, W. Qi, Z. He, Design and mechanisms of antifouling materials for surface plasmon resonance sensors, Acta Biomater. 40 (2016) 100–118, https://doi.org/10.1016/j.actbio.2016.02.035.

[28] L.S. Jung, C.T. Campbell, T.M. Chinowsky, M.N. Mar, S.S. Yee, Quantitative interpretation of the response of surface plasmon resonance sensors to adsorbed films, Langmuir 14 (1998) 5636–5648, https://doi.org/10.1021/la971228b.

[29] M.M. Ouberai, K. Xu, M.E. Welland, Effect of the interplay between protein and surface on the properties of adsorbed protein layers, Biomaterials 35 (2014) 6157–6163, https://doi.org/10.1016/j.biomaterials.2014.04.012.

[30] C. Rodriguez Emmenegger, E. Brynda, T. Riedel, Z. Sedlakova, M. Houska, A. B. Alles, Interaction of blood plasma with antifouling surfaces, Langmuir 25 (2009) 6328–6333, https://doi.org/10.1021/la900083s.

[31] J.E. Gautrot, B. Trappmann, F. Oceguera-Yanez, J. Connelly, X. He, F.M. Watt, W. T.S. Huck, Exploiting the superior protein resistance of polymer brushes to control single cell adhesion and polarisation at the micron scale, Biomaterials 31 (2010) 5030–5041, https://doi.org/10.1016/j.biomaterials.2010.02.066.

[32] R.M. Cornelius, J.G. Archambault, L. Berry, A.K.C. Chan, J.L. Brash, Adsorption of proteins from infant and adult plasma to biomaterial surfaces, J. Biomed. Mater. Res. 60 (2002) 622–632, https://doi.org/10.1002/jbm.10117.

[33] J. Schaller, Human Blood Plasma Proteins ;: Structure and Function, John Wiley & Sons, 2008.

[34] R.W. Caldwell, P.C. Rodriguez, H.A. Toque, S. Priya Narayanan, R.B. Caldwell, Arginase: a multifaceted enzyme important in health and disease,, Physiol. Rev. 98 (2018) 641–665, https://doi.org/10.1152/physrev.00037.2016.

[35] S.M. Steggerda, M.K. Bennett, J. Chen, E. Emberley, T. Huang, J.R. Janes, W. Li, A. L. MacKinnon, A. Makkouk, G. Marguier, P.J. Murray, S. Neou, A. Pan, F. Parlati, M.L.M. Rodriguez, L.A. Van de Velde, T. Wang, M. Works, J. Zhang, W. Zhang, M. I. Gross, Inhibition of arginase by CB-1158 blocks myeloid cell-mediated immune suppression in the tumor microenvironment, J. Immunother, Cancer 5 (2017) 101, https://doi.org/10.1186/s40425-017-0308-4.

[36] M. Czystowska-Kuzmicz, A. Sosnowska, D. Nowis, K. Ramji, M. Szajnik, J. Chlebowska-Tuz, E. Wolinska, P. Gaj, M. Grazul, Z. Pilch, A. Zerrouqi, A. Graczyk-Jarzynka, K. Soroczynska, S. Cierniak, R. Koktysz, E. Elishaev, S. Gruca, A. Stefanowicz, R. Blaszczyk, B. Borek, A. Gzik, T. Whiteside, J. Golab, Small extracellular vesicles containing arginase-1 suppress T-cell responses and promote tumor growth in ovarian carcinoma, Nat. Commun. 10 (2019) 1–16, https://doi.org/10.1038/s41467-019-10979-3.

[37] R. D'Agata, R. Corradini, C. Ferretti, L. Zanoli, M. Gatti, R. Marchelli, G. Spoto, Ultrasensitive detection of non-amplified genomic DNA by nanoparticle-enhanced surface plasmon resonance imaging, Biosens. Bioelectron. 25 (2010) 2095–2100, https://doi.org/10.1016/j.bios.2010.02.008.

[38] G. Grasso, R. D'Agata, L. Zanoli, G. Spoto, Microfluidic networks for surface plasmon resonance imaging real-time kinetics experiments, Microchem. J. 93 (2009) 82–86, https://doi.org/10.1016/j.microc.2009.05.001.

[39] J.S. Shumaker-Parry, C.T. Campbell, Quantitative methods for spatially resolved adsorption/desorption measurements in real time by surface plasmon resonance microscopy, Anal. Chem. 76 (2004) 907–917, https://doi.org/10.1021/ac034962a.

[40] H. Fischer, I. Polikarpov, A.F. Craievich, Average protein density is a molecular-weight-dependent function, Protein Sci. 13 (2009) 2825–2828, https://doi.org/10.1110/ps.04688204.

[41] J. Vörös, The density and refractive index of adsorbing protein layers, Biophys. J. 87 (2004) 553–561, https://doi.org/10.1529/biophysj.103.030072.

[42] S.J. Hurst, A.K.R. Lytton-Jean, C.A. Mirkin, Maximizing DNA loading on a range of gold nanoparticle sizes, Anal. Chem. 78 (2006) 8313–8318, https://doi.org/10.1021/ac0613582.

[43] S. Chen, J. Zheng, L. Li, S. Jiang, Strong resistance of phosphorylcholine self-assembled monolayers to protein adsorption: insights into nonfouling properties of zwitterionic materials, J. Am. Chem. Soc. 127 (2005) 14473–14478, https://doi.org/10.1021/ja054169u.

[44] B. Bilen, Y. Skarlatos, G. Aktas, M.N. Inci, T. Dispinar, M.M. Kose, A. Sanyal, In situ measurement of humidity induced changes in the refractive index and thickness of polyethylene glycol thin films, J. Appl. Phys. 102 (2007) 73534, https://doi.org/10.1063/1.2794708.

[45] Y. Liu, A. Buil, B.C. Collins, L.C.J. Gillet, L.C. Blum, L.-Y. Cheng, O. Vitek, J. Mouritsen, G. Lachance, T.D. Spector, E.T. Dermitzakis, R. Aebersold, Quantitative variability of 342 plasma proteins in a human twin population, Mol. Syst. Biol. 11 (2015) 786, https://doi.org/10.15252/msb.20145728.

[46] L. Wu, J. Jasinski, S. Krishnan, Carboxybetaine, sulfobetaine, and cationic block copolymer coatings: a comparison of the surface properties and antibiofouling behavior,, J. Appl. Polym. Sci. 124 (2012) 2154–2170, https://doi.org/10.1002/app.35233.

[47] W.H. Kuo, M.J. Wang, H.W. Chien, T.C. Wei, C. Lee, W.B. Tsai, Surface modification with poly(sulfobetaine methacrylate-co-acrylic acid) to reduce fibrinogen adsorption, platelet adhesion, and plasma coagulation, Biomacromolecules 12 (2011) 4348–4356, https://doi.org/10.1021/bm2013185.

[48] W. Yang, S. Chen, G. Cheng, H. Vaisocherová, H. Xue, W. Li, J. Zhang, S. Jiang, Film thickness dependence of protein adsorption from blood serum and plasma onto poly(sulfobetaine)-grafted surfaces, Langmuir 24 (2008) 9211–9214, https://doi.org/10.1021/la801487f.

[49] J.E. Krause, N.D. Brault, Y. Li, H. Xue, Y. Zhou, S. Jiang, Photoiniferter-mediated polymerization of zwitterionic carboxybetaine monomers for low-fouling and functionalizable surface coatings, Macromolecules 44 (2011) 9213–9220, https://doi.org/10.1021/ma202007h.

[50] M. Thompson, C. Blaszykowski, S. Sheikh, C. Rodriguez-Emmenegger, A. de los Santos Pereira, Biological Fluid-Surface Interactions in Detection and Medical Devices, Royal Society of Chemistry, 2016, https://doi.org/10.1039/9781782622048.

[51] N. Bellassai, R. D'Agata, V. Jungbluth, G. Spoto, Surface plasmon resonance for biomarker detection: advances in non-invasive cancer diagnosis, Front. Chem 7 (2019) 570, https://doi.org/10.3389/fchem.2019.00570.

[52] S. Dedisch, F. Obstals, A. de los Santos Pereira, M. Bruns, F. Jakob, U. Schwaneberg, C. Rodriguez-Emmenegger, Turning a Killing Mechanism into an Adhesion and Antifouling Advantage, Adv. Mater. Interfaces. 6 (2019) 1900847, https://doi.org/10.1002/admi.201900847.

[53] T. Riedel, Z. Riedelová-Reicheltová, P. Májek, C. Rodriguez-Emmenegger, M. Houska, J.E. Dyr, E. Brynda, Complete identification of proteins responsible for human blood plasma fouling on poly(ethylene glycol)-based surfaces, Langmuir 29 (2013) 3388–3397, https://doi.org/10.1021/la304886r.

[54] P. Akkahat, S. Kiatkamjornwong, S.I. Yusa, V.P. Hoven, Y. Iwasaki, Development of a novel antifouling platform for biosensing probe immobilization from methacryloyloxyethyl phosphorylcholine-containing copolymer brushes, Langmuir 28 (2012) 5872–5881, https://doi.org/10.1021/la204229t.

[55] Q. Liu, W. Li, A. Singh, G. Cheng, L. Liu, Two amino acid-based superlow fouling polymers: poly(lysine methacrylamide) and poly(ornithine methacrylamide), Acta Biomater. 10 (2014) 2956–2964, https://doi.org/10.1016/J.ACTBIO.2014.02.046.

[56] Q. Liu, A. Singh, L. Liu, Amino acid-based zwitterionic poly(serine methacrylate) as an antifouling material, Biomacromolecules 14 (2013) 226–231, https://doi.org/10.1021/bm301646y.

[57] N. Bellassai, A. Marti, G. Spoto, J. Huskens, Low-fouling, mixed-charge poly- l -lysine polymers with anionic oligopeptide side-chains, J. Mater. Chem. B 6 (2018) 7662–7673, https://doi.org/10.1039/C8TB01619D.

[58] M. Svedendahl, S. Chen, A. Dmitriev, M. Käll, Refractometric sensing using propagating versus localized surface plasmons: a direct comparison,, Nano Lett. 9 (2009) 4428–4433, https://doi.org/10.1021/nl902721z.